Melting and interdigitation of microstructured solid supported membranes quantified by imaging ellipsometry

Maja Gedig, Simon Faiß, and Andreas Janshoff[a]

Institute of Physical Chemistry, University of Mainz, Welder Weg 11, 55128 Mainz, Germany

The phase transition of individually addressable microstructured lipid bilayers was investigated by means of noncontact imaging ellipsometry. Two-dimensional membrane compartments were created on silicon substrates by micromolding in capillaries and the phase transition of supported dimyristoylphosphadiylcholine (DMPC) and dipentadecoylphosphatidylcholine (DiC$_{15}$PC) membranes was determined measuring area expansion and thickness of the bilayer as a function of temperature, ethanol concentration, and cholesterol content. Apart from measuring the thermotropic behavior of DMPC on glass slides and silicon wafers, the authors were able to visualize the reversible induction of an interdigitated phase by partitioning of ethanol into the microstructured lipid bilayers. Interdigitation induced by addition of ethanol was measured as a function of cholesterol content and shifts of the main phase transition temperature T_M of microstructured DiC$_{15}$PC were quantified as a function of ethanol concentration. They observed that cholesterol abolishes interdigitation at higher concentrations and found a biphasic behavior of T_M as a function of ethanol concentration in good accordance to what is known from vesicles in solution. © *2008 American Vacuum Society.* [DOI: 10.1116/1.2901179]

I. INTRODUCTION

Today, solid supported membranes are among the most frequently used model systems for complex biological membranes.[1] Although indisputably useful, the solid support itself imposes restrictions that keep researcher busy to circumvent those.[2–8] The number of surface modifications to satisfy the desire to adjust a variety of physical properties is large.[1] Major goals comprise standardized investigations of fundamental biological processes taking place at the plasma membrane such as ion transport across membranes, protein adsorption, and lateral organization of multicomposite membranes.[9–26] However, little is known about the impact of the solid support on physical properties of lipid bilayers attached to surfaces such as the main phase transition temperature or lateral mobility of the lipids. It is expected that phase transitions are strongly affected if not entirely suppressed by the various different supports ranging from glass, gold, silicon, mica to all kinds of functionalized surfaces. Since lateral expansion of the membranes might be restricted or abolished in continuous supported lipid bilayers, microstructured membranes are particular useful to investigate phase changes in bilayers as a function of temperature or membrane active compounds.[27–32]

Recently, we could show using noninvasive imaging ellipsometry of individually addressable microstructured lipid bilayers that the thermotropic phase behavior of bilayers formed from phosphatidylcholines and mixtures with cholesterol is similar to that obtained for multilamellar and vesicular systems.[33] We observed a substantial reduction in cooperativity of the main phase transition, specified by the number of simultaneously melting lipid molecules, and a shift in the main phase transition temperature to higher temperatures by 2–6 °C as a function of the pretreatment of the silicon surface. The lateral mobility of the lipids was found to be essentially identical to that of liposomes at room temperature suggesting that the low cooperativity might be an intrinsic feature of solid supported lipid bilayers.

Besides thermotropic phase transitions lipid bilayers can switch morphology by various other ways. One possibility is the formation of a partly or fully interdigitated phase by multiple amphiphilic molecules such as ethanol, methanol, glycerol, benzyl alcohol, and chlorpromazine.[34–36] From a biological viewpoint, the formation of an interdigitated phase, accompanied by area expansion, thickness decrease, modulation of surface charge density, and the loss of the bilayer midplane should strongly influence the functions of membrane-associated proteins.[36] Therefore, the formation of interdigitated phases in phosphocholine membranes induced by alcohols, in general, and by ethanol, in particular, has been studied extensively by various groups.[34,37–41] Ethanol interacts with PC bilayers in two ways which is frequently referred to as a biphasic behavior. At low concentrations, the main phase transition temperature decreases because interaction of ethanol with the lipids in the fluid phase causes a typical "freezing point depression." At higher concentrations, however, a secondary interaction sets in involving discrete binding sites for ethanol within the head group region of the bilayer in the gel phase. This results in elevation of the phase transition temperature with increasing ethanol concentration and additionally changes the lipid bilayer organization inducing a fully interdigitated phase. The formation of an interdigitated phase is accompanied by an increase of the surface area because water is replaced by larger ethanol molecules. This allows the positioning of the terminal methyl groups

---
[a]Author to whom correspondence should be addressed; Electronic mail: janshoff@mail.uni-mainz.de

from the acyl chains at the bilayer interface region. The unfavorable interactions of the methyl groups with the aqueous phase is counterbalanced by a greater van der Waals interaction of the more closely packed interdigitated acyl chains.

Here, we want to show that it is possible to reversibly induce interdigitation in solid supported bilayers with the same signature as observed for multilamellar systems. As already pointed out by Howland et al.,[42] imaging ellipsometry in conjunction with microstructured lipid bilayers provides an excellent means to investigate both area and thickness changes simultaneously and in a noninvasive fashion.

II. MATERIALS AND METHODS

1,2-dimyristoyl-*sn*-glycero-3-phosphocholine (DMPC) and 1,2-dipentadecoyl-*sn*-glycero-3-phosphocholine (diC15PC) were obtained from Avanti Polar Lipids (Alabaster, AL, USA), methanol, aqueous hydrofluoric acid (35 wt %), and ammonia solution (28%) were from Sigma (Deisenhofen, Germany), aqueous hydrogen peroxide (35 wt %), chloroform, and ethanol were purchased from Carl Roth (Karlsruhe, Germany), and tris(hydroxymethyl) aminomethane hydrochloride (Tris/HCl) and sodium chloride were from Fluka (Neu Ulm, Germany). TexasRed-1,2-dihexadecyl-sn-glyerco-3-phosphoethanolamine (TexasRed DPHE) was purchased from Molecular Probes (Eugene, USA). All chemicals were high grade and used without further purification. Poly(dimethylsiloxane) (PDMS) (Sylgard 184) was obtained from DowCorning (Midland, MI, USA). Polished prime silicon wafers were from Wacker Siltronic (Munich, Germany) and Optislides™, which are glass slides (BK7) with high refractive index ($n=2.348$) due to an intermediate Ta_2O_5 layer with a nominal thickness of 80–90 nm and an uppermost SiO_2 film of approximately 8–10 nm, were purchased from Nanofilm Technology (Göttingen, Germany).

A. Formation of structured lipid bilayers

Individually addressable microstructured solid-supported lipid bilayers were prepared by micromolding in capillaries, as previously described.[29–32] In brief, all preparation steps were carried out at 40 °C, i.e., well above the main phase transition temperature of DMPC (23 °C) and DiC$_{15}$PC (33 °C). The silicon wafers were cleaned with diluted aqueous HF solution (1% v/v) and activated in $NH_4OH/H_2O_2/H_2O$ (1:1:5, v/v) at 75 °C for 20 min. This process simultaneously generates a thin SiO_2 layer. The oxidized wafers were stored in water and used on the same day. Optislides™ were also treated with $NH_4OH/H_2O_2/H_2O$ (1:1:5, v/v) at 75 °C for 20 min rendering the surface extremely hydrophilic. Optislides™ with a sandwich structure of Ta_2O_5 (88 nm) followed by a thin layer of SiO_2 (8 nm). Cleaning does not affect the thickness of the Ta_2O_5 layer but reduces the SiO_2 adlayer thickness to merely 2 nm. The PDMS molds serving as the microfluidic network to deposit the separated bilayer structures were cleaned in oxygen plasma for 2 min (Plasma Cleaner, Harrick, NY, USA) and then placed on dry silicon wafers/Optislides™. The capillaries formed by the PDMS mold and the silica surface were filled with 0.3 μl of a suspension of unilamellar vesicles. By vesicle adsorption inducing rupture and spreading to form planar lipid bilayers confined to the capillary, membrane stripes consisting of various lipid compositions were obtained.[29,31] After 10 min, buffer was added to the PDMS channels on the silica surface to form a liquid film surrounding the stamp. Subsequently, the PDMS network was gently peeled off and the surface was extensively rinsed with buffer to remove remaining vesicles. Without drying the surface the wafer was transferred to the ellipsometry measuring cell. Figure 1 schematically displays the preparation of individually addressable microstructured lipid bilayers on solid supports together with a confocal laser scanning micrograph (Leica TCS SL, Leica Microsystems, Bensheim, Germany) that shows the nicely separated bilayer stripes exhibiting a width of 15 μm separated by membrane free spacings of 5 μm employing 1 mole % of TexasRed DHPE as a label.

B. Ellipsometry

A commercially available imaging ellipsometer (EP^3-SW, Nanofilm Technologie, Göttingen, Germany) equipped with a Nd doped yttrium aluminum garnet laser ($\lambda=532$ nm) was used to determine thickness and area of the structured lipid membranes. Data acquisition and analysis have been previously described in great detail.[33]

III. RESULTS AND DISCUSSION

A. Thermotropic phase transition of microstructured DMPC bilayers

In the following section, we will briefly review and add new data on temperature controlled ellipsometric experiments with microstructured DMPC bilayers deposited on SiO_2 adlayers of silicon wafers and optical dense glass slides (Optislides™). Starting from low temperature, the membrane compartments are heated up in small increments. After thermal equilibration, which takes usually about 10 min, a "delta map" of the entire image, as exemplarily shown in Fig. 2, is recorded and transformed into a "thickness map" by applying the corresponding optical model as detailed elsewhere.[33] Notably, due to optical anisotropy of the bilayer, we rather use relative changes in thickness $\Delta d/d$ than absolute heights.[43] However, the ellipsometrically determined thickness values obtained from the isotropic optical model correspond very well with the height determined from atomic force microscopy (AFM) images of the same sample.[30] Figure 3 shows the change of relative bilayer thickness and bilayer area with temperature during the discrete heating process. On average, the bilayer thickness is reduced from 4.6 to 3.2 nm and the bilayer area simultaneously increased by 26% during the phase transition. This is in perfect agreement with earlier findings employing multilamellar systems (vesicles and supported multilayers).[44] For instance, Nagle et al.[45] found 3.6 nm for the bilayer in the fluid state, while Tokumasu et al.[46] reported an average thickness of 4.3 nm for gel phase and 3.4 nm for fluid phase DMPC bilayers.
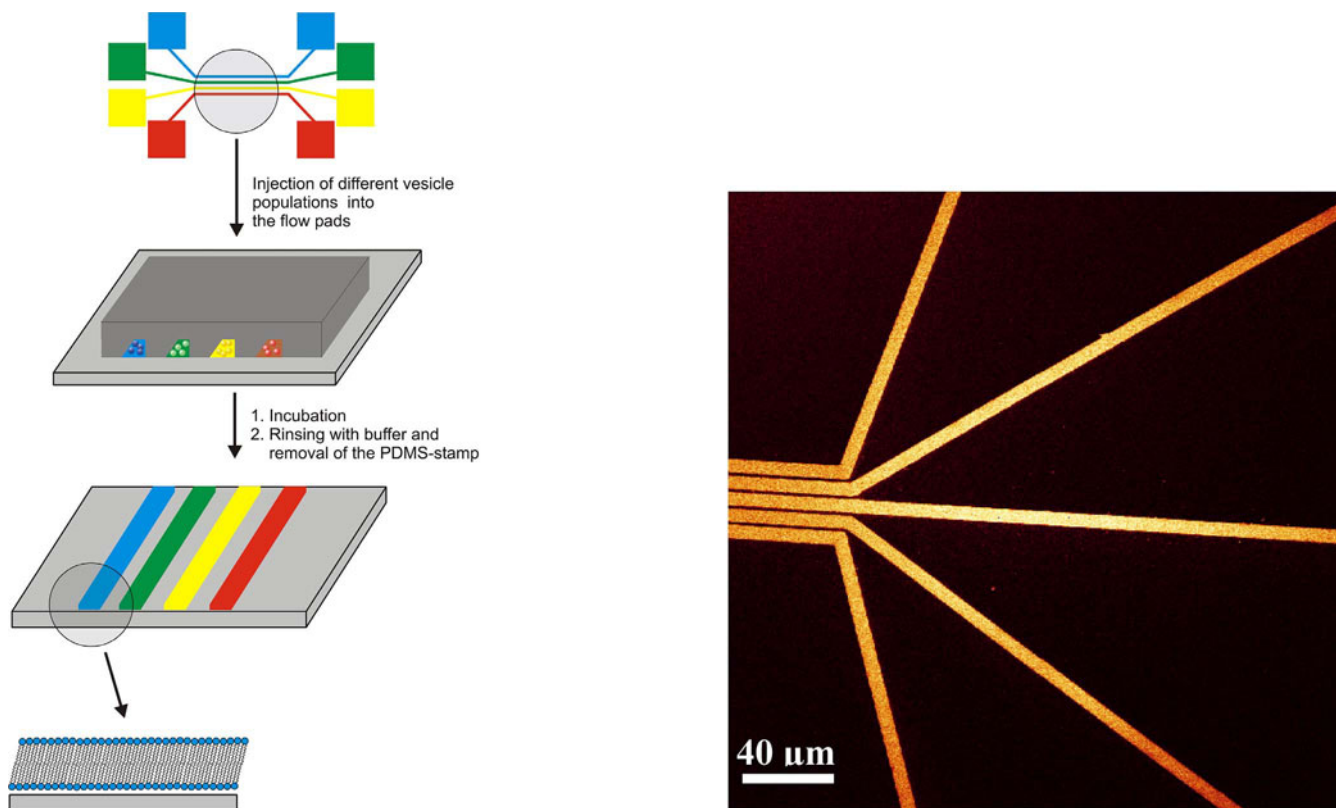
FIG. 1. (A) Preparation of microstructured lipid bilayers on solid supports by means of micromolding in capillaries. (B) Confocal laser scanning micrograph of microstructured DMPC bilayers labeled with 0.5 mole % Texas Red DHPE on glass.
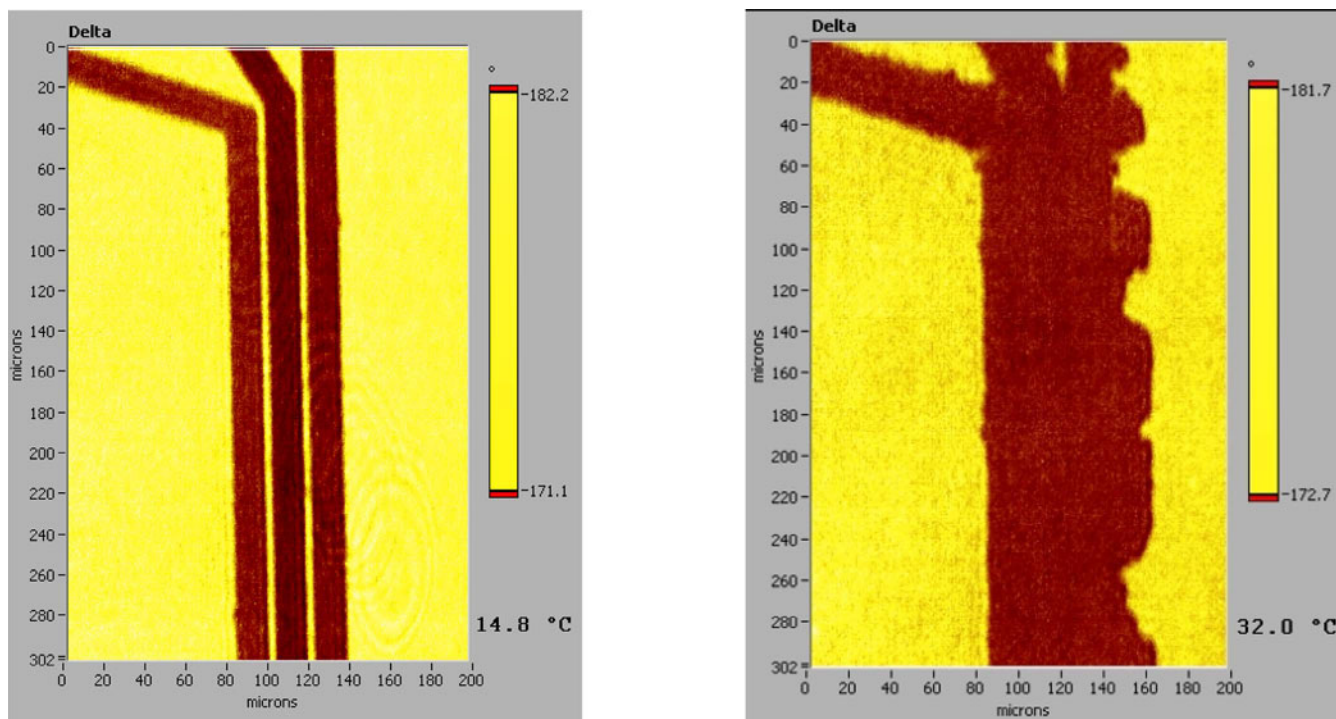
FIG. 2. Ellipsometry of microstructured DMPC compartments. Delta map of three DMPC membrane stripes (dark) on silicon (bright) before heating (left) at 14.8 °C and above the main phase transition temperature at 32 °C (right).
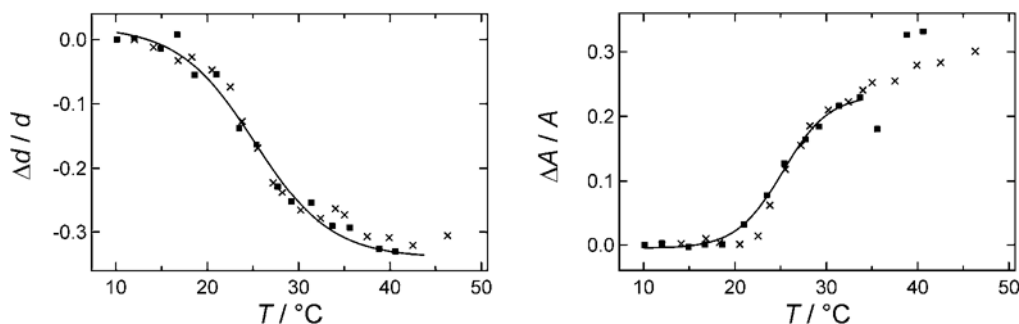
FIG. 3. Change in relative thickness (A) and area (B) of DMPC membrane stripes deposited on either Optislides™ (■) or silicon wafers (×).

Heating and cooling curves show a hysteresis of about 2 °C to lower temperatures in the cooling cycle (data not shown). The phase transition temperature is determined by application of an empirical sigmoidal fit to the data.[30] From the thickness change with temperature, we obtain T_m =25.0 ± 0.3 °C upon heating and from the area expansion T_m=26.7 ± 0.4 °C. Considering that the transition is rather broad the two values correspond reasonably well. Both curves show a broad transition within a regime of about 11 °C. The whole process is reversible, i.e., heating the sample a second time leads to the same values for thickness and area (data not shown). These numbers are comparable to values found by AFM measurements of a structured bilayer on glass,[30] but slightly higher than the transition temperature found for multilamellar vesicles. The broadness of the transition, which is reported as 2 °C for multilamellar and 7 °C for unilamellar vesicles hints to a lower cooperativity of phase transition when the membranes are attached to a solid support.[47,48] In fact, the temperature scan of microstructured membranes corresponds to a cooperativity unit of around 10 rather than more than 100, as obtained for multilamellar vesicles.[48,49] However, lateral mobility of the membranes as shown by fluorescence recovery after photobleaching is preserved on the silicon substrate as compared to liposomes.[33,50]

Interestingly, the two different samples prepared either on Optislides™ or on silicon wafers exhibited a nearly identical temperature profile, suggesting that variations in the thermotropic behavior are negligible as long as the same type of surface, SiO_2 in this case, is used. However, examination of the same sample on two consecutive days or using silicon wafers that were oxidized 2 days before as compared to freshly oxidized ones leads to nonsystematic variations of T_m between 24.5 and 30.2 °C (data not shown). Hence, it is recommended using freshly prepared surfaces to obtain reliable results. These findings might also explain the frequently observed differences in T_m.[46,51–54] In order to rule out that variation in surface quality accounts for inconsistent results on the thermotropic properties of membranes, it is inevitable to provide an internal standard, i.e., a membrane of known thermomechanical properties. This is one of the greatest benefits of individually addressable microstructured bilayers in the way we prepare them here since two stripes of different composition can be deposited adjacent to each other, which allows us to use one membrane stripe as the internal stan-

dard, while the others can be varied in composition. In conjunction with imaging ellipsometry, atomic force or fluorescence microscopy, this approach provides the possibility to monitor thickness and area changes of various solid supported bilayers almost simultaneously.

B. Interdigitation of DMPC bilayers induced by the addition of ethanol

The main focus of this study lies on the reversible interdigitation of phosphatidylcholine induced by addition of ethanol above the phase transition temperature and subsequent cooling below T_M. Figures 4(a)–4(d) show ellipsometric thickness maps and corresponding height profiles of a structured DMPC membrane at various temperatures and conditions. At 22 °C, the five stripes are nicely separated and show a height of 4.5 ± 0.2 nm (A); after heating the sample to 40 °C, the thickness is reduced to 3 nm and the stripes are expanded, but still separated (B). Then, the sample was rinsed with buffer/ethanol at 40 °C for 30 min. The ethanol concentration was 3.5M, i.e., well above the reported threshold for full interdigitation in multilamellar vesicles. The threshold for full interdigitation was reported to be 1.84M for multilamellar vesicles by Rowe.[37] As a consequence, membrane thickness is further reduced to 2.5 nm and due to the substantial area expansion of the membrane the stripes are no longer separated (C). After cooling the sample below the phase transition temperature, the membrane stripes exhibit a height of 3.2 ± 0.2 nm, which is considerably lower than in the absence of ethanol in the beginning of the experiment (A), indicating the formation of an interdigitated phase (D). Reversibility of the process is demonstrated by heating the sample again to 40 °C accompanied by thorough rinsing with pure buffer for 45 min to remove the ethanol within the bilayer. Figure 4(e) shows that a bilayer thickness of 3 nm is regained, and after cooling the sample to 18 °C, the morphology of the membrane stripes is almost fully recovered. The membrane stripes are clearly visible and display a bilayer height of 4.5 nm (F). The various steps are summarized in Fig. 5, in which the thickness of the bilayer is shown for each reaction step.

Interestingly, in most cases the shape of the stripes is preserved even after the membranes form an apparently continuous bilayer. We attribute this fact to the different surface
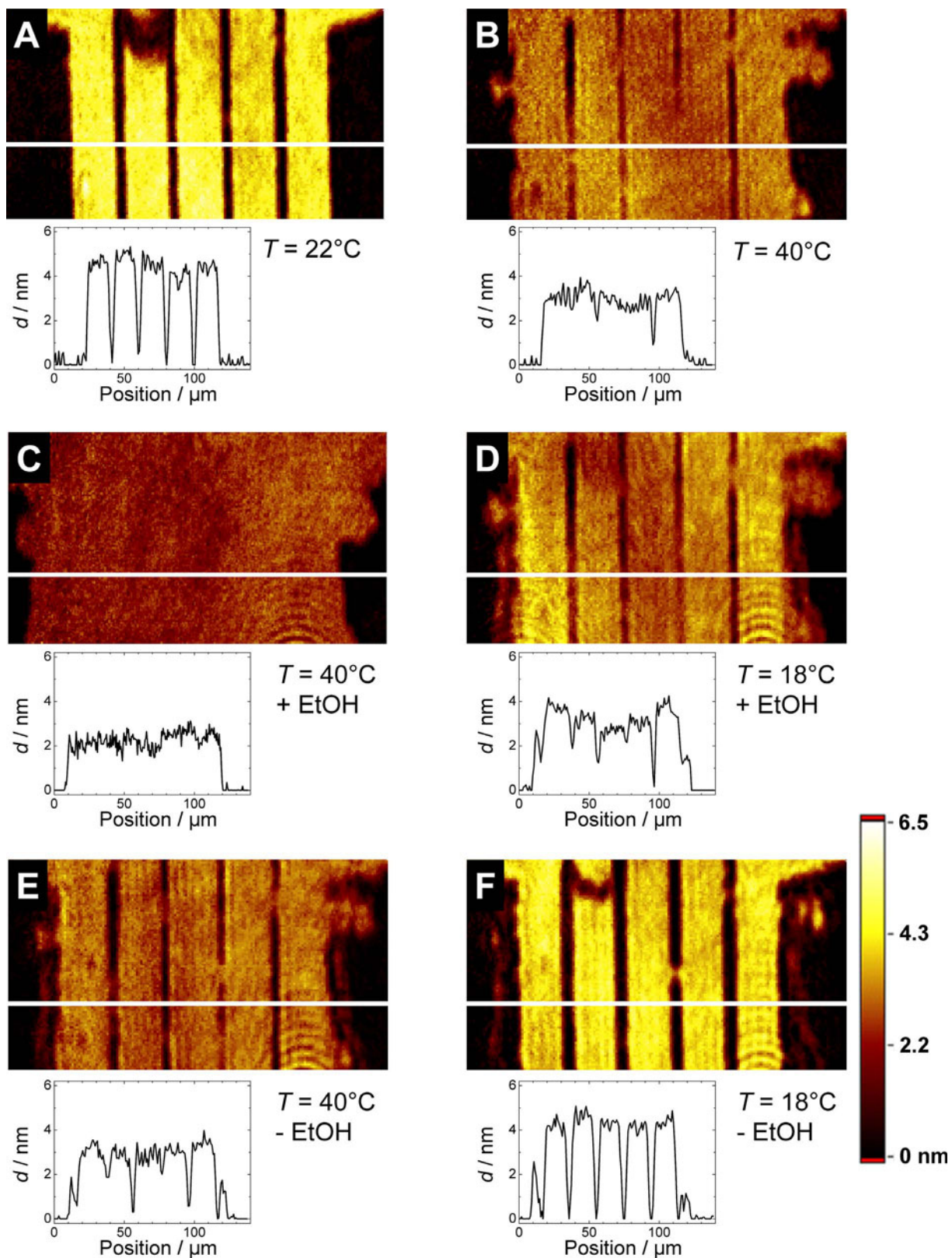
FIG. 4. Ellipsometric thickness maps (140×80 μm^2) of structured DMPC bilayer stripes on SiO$_2$/Si substrate in buffer and buffer/ethanol (4:1 v/v) below and above the main phase transition temperature. The white line indicates the position of the height profile shown below the images. The height scale is valid for all images. (A) $T=22\,^\circ C$, buffer, (B) $T=40\,^\circ C$, buffer, (C) $T=40\,^\circ C$, with ethanol, (D) $T=18\,^\circ C$, with ethanol, (E) $T=40\,^\circ C$, after rinsing with pure buffer, and (F) $T=18\,^\circ C$, buffer.
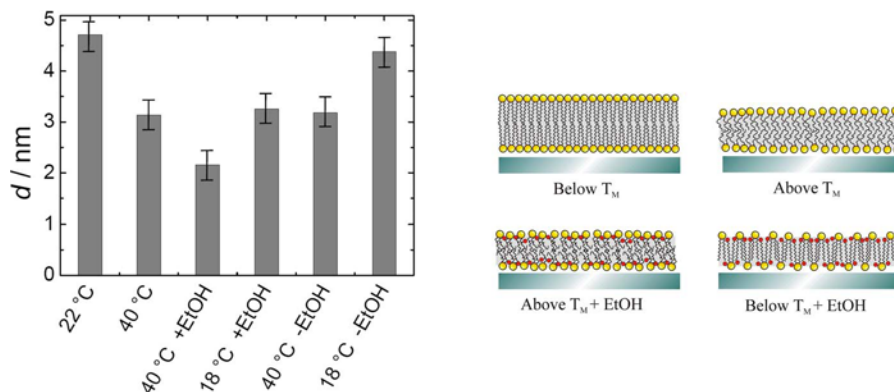
FIG. 5. Change of DMPC-bilayer thickness as a function of temperature and ethanol addition(+)/removal(-) as measured by ellipsometry (Figure 4).

properties of the membrane free region, which has been in contact with a PDMS stamp and hence display different surface energies than the area which has been coated with the bilayer. Even a defect in the membrane as visible in Fig. 4(a) that was healed while heating and formation of the interdigitated phase reappears at 18 °C after removal of ethanol. This shows that marginal changes on the surface of the solid support strongly influence the formation, stability and adhesion of solid supported membranes.

Miszta et al.[55] recently claimed that interdigitation due to insertion of ethanol does not take place in solid supported bilayer originating from vesicle spreading. However, the authors used bilayers in the fluid state such as DOPC/DOPS and neat DOPC, which is different from our study but still in correspondence with the literature on liposomes.[34,37,56]

C. Interdigitation of DMPC as a function of cholesterol content

Figure 6 exemplarily shows the impact of cholesterol on the extend of interdigitation induced by ethanol added to DMPC-bilayer stripes at a concentration of 20% (v/v) mixed with buffer (0.2M Tris/HCl, 0.1M NaCl, 1 mM NaN$_3$, pH 7.4). On the left hand side of Fig. 6, the general experimental sequence is shown, which comprises ethanol partition between bilayer and solution at elevated temperature ($>T_M$), cooling the sample under T_M to induce interdigitation, and eventually removal of ethanol by rinsing with pure buffer at temperatures higher than T_M. At moderate cholesterol content (<5 mole %), we measure the typical signature of interdigitation, i.e., a decreased thickness accompanied by an increased area of the bilayer. At high cholesterol content (>30 mole %), essentially no impact of ethanol either on lateral area or on the thickness of the bilayer was observed. We found that up to a cholesterol content of 5 mole % interdigitation of the bilayer is actually enhanced. At higher concentrations of cholesterol than 5 mole %, however, interdigitation diminishes to zero in a linear fashion with increasing amount of cholesterol (Fig. 7). Importantly, the effect of ethanol is reversible if samples are rinsed with pure buffer at temperatures higher than the main phase transition temperature of the membrane (reaction step IV–V). These findings

correspond well to what is known from literature employing PC/cholesterol liposome suspensions.[57] Even the slightly enhanced effect of ethanol on the bilayers' thickness decrease/ area increase at 5 mole % cholesterol as compared to neat DMPC has also been observed for liposomes. Hence, we can conclude that solid supported bilayers display a similar phase behavior than liposomes in suspension. Notably, the reaction cycle is fully reversible showing essentially the same relative area and thickness changes in steps IV and I as well as V and the initial state at 18 °C in the absence of ethanol (data not shown).

D. Influence of ethanol concentration on the main phase transition temperature of diC$_{15}$PC bilayers

It is known that ethanol influences the main phase transition temperature of lipid bilayers in biphasic fashion.[34,35,37,56] At ethanol concentrations below 60 mg/ml, the main phase transition temperature of phosphatidylcholines decreases, which can be explained in terms of an increased solubility of ethanol in the fluid phase as compared to the gel phase (freezing point depression). At 60 mg/ml, however, a fully interdigitated phase is reached and the binding capability for ethanol is substantially increased due to the presence of nonpolar groups close to the head group region. This enhanced solubility of ethanol is responsible for an increase in T_M, as described in detail by Rowe and co-workers.[34,35,37,56] Here, we used microstructured PC bilayers with saturated C$_{15}$ chains rendering T_M ($T_M=33$ °C in the absence of ethanol) in an experimentally easily accessible regime. We performed cooling cycles (from high to low temperature) starting with a defined ethanol concentration in solution and appropriate equilibration times >1 h [Fig. 8(a)]. Figure 8(b) shows the main phase transition temperature measured by recording cooling cycles with imaging ellipsometry as a function of ethanol concentration in solution. A clear biphasic behavior was found as reported by Rowe for liposome suspensions. The minimum of T_M was found closely to 60 mg/ml, while saturation of the interdigitated bilayer with ethanol was reached at 130 mg/ml.
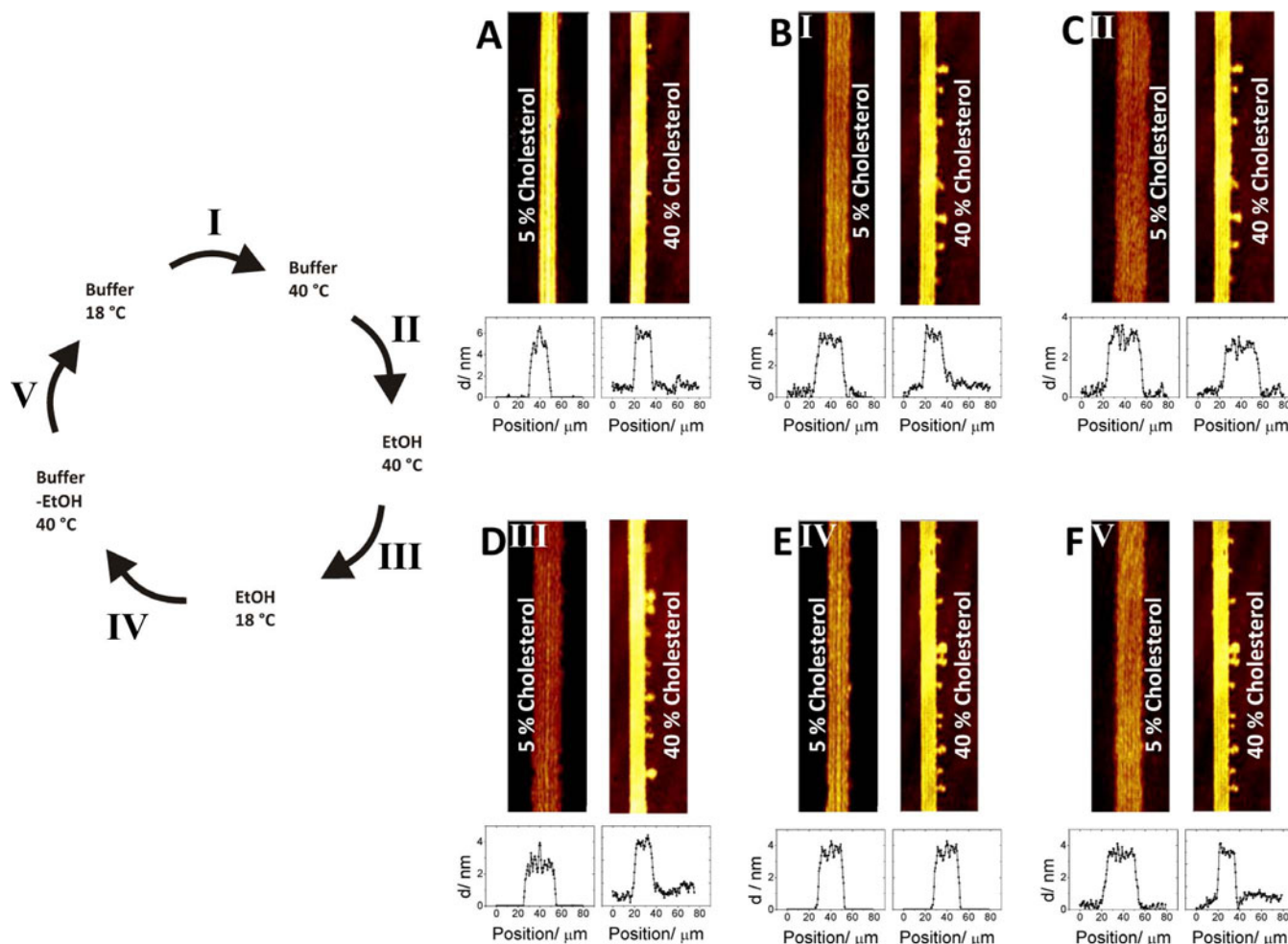
FIG. 6. Left: sequence of experiments. [(A)–(F)] Thickness maps with representative line scans from imaging ellipsometry of structured DMPC bilayers with 5 and 40 mole % cholesterol taken at the denoted experimental steps (I–V).

In summary, even this subtle effect of ethanol concentration on T_M could be reproduced by using solid supported membranes providing strong evidence that SSM display essentially the same phase behavior than bilayers organized in liposomes.

IV. CONCLUSIONS

The influence of the solid support on the phase behavior of DMPC has been quantitatively investigated by noninvasive imaging ellipsometry in combination with microstructured lipid bilayers. We found that careful sample preparation leads to reproducible results in terms of phase transition temperature and broadness of the transition. Although the main phase transition temperature is only slightly shifted to higher temperature cooperativity of the thermotropic transition is substantially reduced. Ethanol induced interdigitation with single lipid bilayers attached to a silicon wafer could be visualized by imaging ellipsometry and was shown to be a reversible process. Also, the more subtle phase behavior such as the impact of cholesterol on the formation of interdigitated lipid structures gend the dependency of T_M on the ethanol concentration could be reproduced with solid supported bi-
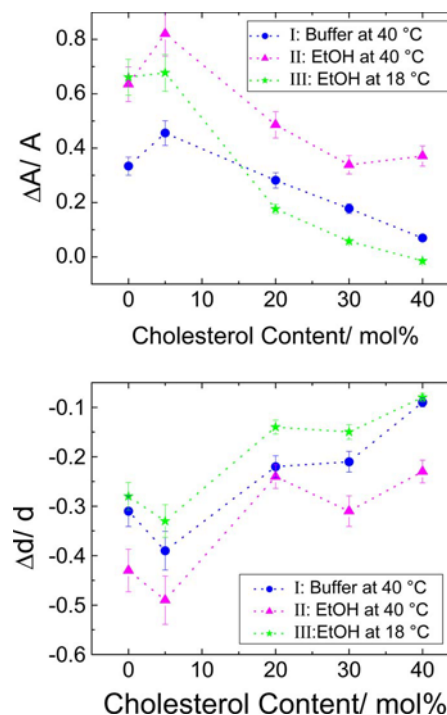
FIG. 7. Relative area (top) and thickness (bottom) changes as a function of cholestrol content for the first three reaction steps (I–III).
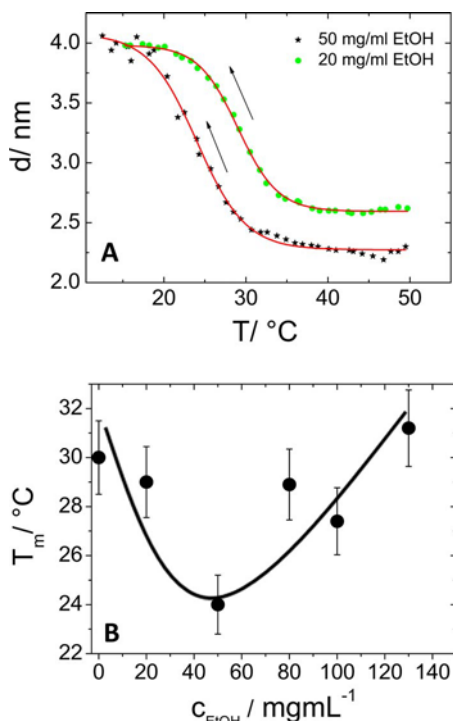
FIG. 8. (A) Temperature scans from high to low temperature (arrows) of microstructured DiC$_{15}$PC bilayers within different ethanol/buffer solutions. Additin of 20 mg/ml ethanol yields in a T_M of 29 ± 0.5 °C, while a concentration of 50 mg/ml results in a T_M of 24 ± 0.5 °C. (B) Dependency of the main phase transition temperature of DiC$_{15}$PC bilayers on the ethanol concentration in solution. The spline indicated the biphasic behavior.

layers. Both area and thickness changes could be simultaneously determined at each reaction step and the results are in good accordance with previous findings employing liposomes.

ACKNOWLEDGMENTS

[1] A. Janshoff and C. Steinem, Anal. Bioanal. Chem. **385**, 433 (2006).
[2] M. Tanaka and E. Sackmann, Nature (London) **437**, 656 (2005).
[3] E. Reimhult, F. Höök, and B. Kasemo, Langmuir **19**, 1681 (2003).
[4] E. Reimhult, M. Zäch, F. Höök, and B. Kasemo, Langmuir **22**, 3313 (2006).
[5] F. Richter, G. Rapp, and L. Finegold, Phys. Rev. E **63**, 051914 (2001).
[6] R. P. Richter and A. R. Brisson, Biophys. J. **88**, 3422 (2005).
[7] R. P. Richter, N. Maury, and A. R. Brisson, Langmuir **21**, 299 (2005).
[8] H. Schönherr, J. M. Johnson, P. Lenz, C. W. Frank, and S. G. Boxer, Langmuir **20**, 11600 (2004).
[9] K. Ataka, F. Giess, W. Knoll, R. Naumann, B. Haber-Pohlmeier, Richter, and J. Heberle, J. Am. Chem. Soc. **126**, 16199 (2004).
[10] V. Atanasov, N. Knorr, R. S. Duran, S. Ingebrandt, A. Offenhäusser, W. Knoll, and I. Koeper, Biophys. J. **89**, 1780 (2005).
[11] M. A. Cooper, J. Mol. Recognit. **17**, 286 (2004).
[12] B. A. Cornell, V. L. B. Braach-Maksvytis, L. G. King, P. D. J. Osman, L. Wieczorek, B. Raguse, and R. J. Pace, Nature (London) **387**, 580 (1997).
[13] J. Drexler and C. Steinem, J. Phys. Chem. B **107**, 11245 (2003).
[14] G. Elender, M. Kühner, and E. Sackmann, Biosens. Bioelectron. **11**, 565 (1996).
[15] G. Favero, L. Capanella, S. Cavallo, A. D'Annibale, M. Perrella, E. Mattei, and T. Ferri (unpublished).
[16] K. Fendler, M. Klingenberg, G. Leblanc, J. J. H. H. M. DePont, B. LKelety, W. Dörner, and E. Bamberg, in *Ultrathin Electrochemical Chemo- and Biosensors*, edited by V. M. Mirsky (Springer, Berlin, 2004), pp. 331–349.
[17] F. Giess, M. G. Friedrich, J. Heberle, R. L. Naumann, and W. Knoll, Biophys. J. **87**, 3213 (2004).
[18] M. Goryll, S. J. Wilk, G. M. Laws, T. J. Thornton, S. M. Goodnick, M. Saranti, J. Tang, and R. S. Eisenberg, Superlattices Microstruct. **34**, 451 (2003).
[19] S. Gritsch, P. Nollert, F. Jähnig, and E. Sackmann, Langmuir **14**, 3118 (1998).
[20] W. Knoll, K. Morigaki, R. Naumann, B. Sacca, S. Schiller, and E.-K. Sinner, in *Ultrathin Electrochemical Chemo- and Biosensors*, edited by V. M. Mirsky (Springer, Berlin, 2004), pp. 239–253.
[21] H. Lang, C. Duschl, and H. Vogel, Langmuir **10**, 197 (1994).
[22] C. Steinem, H.-J. Galla, and A. Janshoff, Phys. Chem. Chem. Phys. **2**, 4580 (2000).
[23] C. Steinem, A. Janshoff, H.-J. Galla, and S. Manfred, Bioelectrochem. Bioenerg. **42**, 213 (1997).
[24] C. Steinem, A. Janshoff, W.-P. Ulrich, M. Sieber, and H.-J. Galla, Biochim. Biophys. Acta **1279**, 169 (1996).
[25] C. Steinem, A. Janshoff, K. von dem Bruch, K. Reihs, J. Goossens, and H.-J. Galla, Bioelectrochem. Bioenerg. **45**, 17 (1998).
[26] T. Stora, J. H. Lakey, and H. Vogel, Angew. Chem., Int. Ed. **38**, 389 (1999).
[27] T. Yang, S.-Y. Jung, H. Mao, and P. S. Cremer, Anal. Chem. **73**, 165 (2001).
[28] M. a. Holden, S.-Y. Jung, T. Yang, E. T. Castellana, and P. S. Cremer, J. Am. Chem. Soc. **126**, 6512 (2004).
[29] A. Janshoff and S. Künneke, Eur. Biophys. J. **29**, 549 (2000).
[30] S. Schuy and A. Janshoff, ChemPhysChem **7**, 1207 (2006).
[31] S. Künneke and A. Janshoff, Angew. Chem., Int. Ed. **41**, 314 (2002).
[32] S. Schuy and A. Janshoff, J. Colloid Interface Sci. **295**, 93 (2006).
[33] S. Faiß, S. Schuy, D. Weiskopf, C. Steinem, and A. Janshoff, J. Phys. Chem. B **111**, 13979 (2007).
[34] E. S. Rowe, Biochemistry **22**, 3299 (1983).
[35] S. A. Simon and T. J. McIntosh, Biochim. Biophys. Acta **773**, 169 (1984).
[36] J. L. Slater and C.-H. Huang, Prog. Lipid Res. **27**, 325 (1988).
[37] E. S. Rowe, Biochim. Biophys. Acta **813**, 321 (1985).
[38] J. Mou, J. Yang, C. Huang, and Z. Shao, Biochemistry **33**, 9981 (1994).
[39] J. M. Sturtevant, Proc. Natl. Acad. Sci. U.S.A. **79**, 3963 (1982).
[40] L. Löbbecke and G. Cevc, Biochim. Biophys. Acta **1237**, 59 (1995).
[41] N. Pappayee and A. K. Mishra, Photochem. Photobiol. **73**, 573 (2001).
[42] M. C. Howland, A. W. Szmodis, B. Sanii, and A. N. Parikh, Biophys. J. **92**, 1306 (2007).
[43] Z. Salamon and G. Tollin, Biophys. J. **80**, 1557 (2001).
[44] T. Heimburg, Biochim. Biophys. Acta **1415**, 147 (1998).
[45] J. F. Nagle, R. Zhang, S. Tristram-Nagle, W. Sun, H. I. Petrache, and R. M. Suter, Biophys. J. **70**, 1419 (1996).
[46] F. Tokumasu, A. J. Jin, and J. A. Dvorak, J. Electron Microsc. **51**, 1 (2002).
[47] P. W. M. Van Dijck, B. De Kruijff, P. A. M. M. Aarts, A. J. Verkleij, and J. De Gier, Biochim. Biophys. Acta **506**, 183 (1978).
[48] D. Marsh, A. Watts, and P. F. Knowles, Biochim. Biophys. Acta **465**, 500 (1977).
[49] G. Cevc and D. Marsh, *Phospholipid Bilayers: Physical Principles and Models* (Wiley-Interscience, New York, 1987).
[50] N. Kahya and P. Schwille, J. Fluoresc. **16**, 671 (2006).
[51] F. Yarrow, T. J. H. Vlugt, J. P. J. M. van der Eerden, and M. M. E. Snel, J. Cryst. Growth **275**, e1417 (2005).
[52] A. Charrier and F. Thibaudau, Biophys. J. **89**, 1094 (2005).
[53] Z. V. Leonenko, E. Finot, H. Ma, T. E. S. Dahms, and D. T. Cramb, Biophys. J. **86**, 3783 (2004).
[54] A. F. Xie and S. Granick, Nat. Mater. **1**, 129 (2002).
[55] A. Miszta, B. van Deursen, R. Schoufs, M. Hof, and W. T. Hermens, Langmuir **24**, 19 (2008).
[56] E. S. Rowe and J. M. Campion, Biophys. J. **67**, 1888 (1994).
[57] C. Trandum, P. Westh, K. Jorgensen, and O. G. Mouritsen, Biophys. J. **78**, 2486 (2000).